

Scientific Session 1

Pathology & Radiology Imaging Abstracts

(running concurrently with Scientific Session 2)
(Grand Ballroom 4)

Virtual Reality Powerwall Versus Conventional Microscope: Comparison of Efficiency and Diagnostic Behaviour

Darren E. Treanor, MB BSc, MD¹ (darrentreanor@nhs.net), Naomi Jordan-Owers, MD¹, John Hodrein, BSc², Jason Wood², PhD, Phil Quirke, MD, PhD¹, Roy Ruddle, PhD²; ¹Pathology and Tumour Biology, ²School of Computing, University of Leeds, Leeds, United Kingdom

Content:

We describe the implementation of a 50 megapixel virtual reality Powerwall for viewing virtual slides, and compare it with a conventional microscope. Efficient patterns of use of the system are identified to help in future system development.

Technology:

Virtual slides are enormous digital images, and navigating them with a conventional desktop display can be inefficient. We have developed a virtual slide viewing system using a 50 megapixel, 3.5m x 1.5m, tiled display called a virtual reality Powerwall, aiming to increase diagnostic efficiency.

Design:

8 pathologists performed a set of 4 diagnostic tasks on the conventional microscope and Powerwall, with their actions recorded by video. Diagnostic confidence and time to complete the task was measured. A secondary analysis of diagnostic efficiency using the Powerwall was undertaken by reviewing experimental videos and assigning a subjective efficiency score to the task (e.g. subjects who made use of physical rather than virtual navigation, or who stood close enough to the device to utilize the increased resolution were marked as using the device efficiently).

Results:

Diagnostic time was similar for the conventional microscope and the Powerwall (87.8 vs 88.7 sec), as was diagnostic confidence (90 vs. 89%). Mean fixation time was longer with the Powerwall than the microscope (1.4 vs. 0.9s, $P < 0.01$), reflecting the relatively larger tissue area viewed at once with the Powerwall. Subjects panned and zoomed less with the Powerwall than the microscope (total 1812 vs. 2910 pans and 193 vs. 246 zooms for all tasks). Further analysis of interaction with the Powerwall device found that subjects used it efficiently in 58%

of tasks, despite their lack of familiarity with the device. Inefficient users tended to take more steps, and make more pan and zoom actions. Efficient use was associated with reduced time to complete certain tasks.

Conclusions:

Virtual slides can be viewed efficiently and with diagnostic confidence using a Powerwall display. Using a Powerwall alters viewing methods compared to a microscope. Efficient use of the device in a subset of tasks reveals potential for further improvements with megapixel devices.

Geometric Approaches For Cancer Detection and Classification Based on Nuclear Structure

Wei Wang, MS (wwang2@andrew.cmu.edu), John A. Ozolek, MD Dejan Slepcev, PhD, Gustavo K. Rohde, PhD; Carnegie Mellon University, Pittsburgh, PA

Context:

Visual interpretation of histopathology images is the most common method used in diagnostic pathology. Many lesions, both benign and malignant, can be difficult to distinguish from one another based solely on histomorphological grounds and expensive studies may be required. Our study shows that geometric approaches are superior to feature-based methods for discriminating between differential diagnoses in certain pediatric liver tumors and thyroid tumors based on nuclear structure (size, shape, chromatin pattern) from digital images.

Technology:

Nuclear segmentation from digital images is performed using a hybrid level set and graph cut method. Classification is performed by quantifying similarities in a group of nuclei to groups of nuclei in a trained database. Group (distribution) distances are computed using novel geometric approaches (based on optimal transportation distances) as well as more commonly used numerical features.

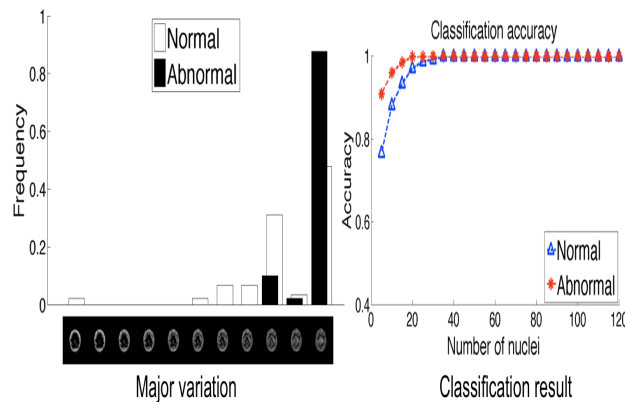
Design:

Analysis was performed on 9 cases of normal and cancers (five hepatoblastoma, two thyroid follicular adenoma and two follicular carcinoma). Representative fields of Feulgen stained sections from routinely processed tissues were imaged at 1000X

magnification. Our geometric approaches are able to automatically classify this data with 100% accuracy using both case-based and randomized blindfolded cross validation strategies.

Results:

The figure (right) shows the detection rate for normal and hepatoblastoma as a function of number of nuclei used to perform classification (40 nuclei are needed for perfect classification accuracy). The histogram (left) represents the number of nuclei in each population (normal vs. hepatoblastoma) most similar to the geometric path (provided by the optimal transportation metric) shown at the bottom. The figure also indicates that it is uncommon for hepatoblastoma nuclei to have chromatin concentrated around the edge of the nucleus.



Conclusions:

We propose a novel computer-assisted method for cancer detection and classification based on quantifying distributions of nuclei over mathematical geometries. Validation of our approach with the test data available demonstrated that our methods can distinguish between normal liver and hepatoblastoma and follicular adenoma and follicular carcinoma with 100% accuracy. In addition, our approach can be used to define unique nuclear "signatures" for individual tissues and lesions.

Tissue Fold Detection and Image Quality in Whole Slide Imaging

Pinky A. Bautista (pbautista@partners.org),
 Yukako Yagi; Department of Pathology,
 Massachusetts General Hospital, Boston, MA

Context:

In whole slide imaging the resulting image quality is dependent on several factors such as the optics specifications, hardware and software features of the imaging device, and the quality of the tissue slide itself. It has been observed that the presence of tissue artifacts in a slide can affect the quality of the scanned image, specifically some tissue areas, aside from areas occupied by the tissue artifacts, appear blurred.

Technology:

The main objective of this work is to develop an algorithm to detect tissue artifacts from the thumbnail version of a whole slide image. For this report however, we specifically focus on the detection of tissue folds wherein we proposed an enhancement scheme that utilizes the saturation and luminance components of the pixels as shifting factors to the original color values to localize the presence of folds.

Design:

The fold detection algorithm was applied to the low pixel resolution of the high resolution whole slide, i.e. 14.6 $\mu\text{m}/\text{pixel}$. To probe the usefulness of the algorithm, we compared the image quality of the images produced by scanning in automated and manual modes. In the 'automated' mode the fold areas may be selected as focus points by the scanner whereas in manual mode tissue folds are avoided in the selection of the focus points by referring to the resulting enhanced image wherein the location of tissue folds are emphasized.

Results:

To show the viability of the proposed enhancement algorithm in detecting tissue folds, the slides were scanned at 0.43 $\mu\text{m}/\text{pixel}$ resolution in manual and automatic modes. Visual comparisons of specific tissue areas from whole slide images produced by automatic and manual modes show that with the manual selection of focus points the resulting images are sharper and not blurry.

Conclusions:

It has been shown in the results of our experiments that referring to the enhanced image, where tissue folds are highlighted, to avoid the tissue artifacts in selecting the focus points helps improve the resulting image quality. Thus, incorporating the proposed enhancement scheme to detect tissue folds to the scanning procedure will effectively increase the efficiency of the scanning devices.

H&E Digital Staining From the Multispectral Image of a Specimen Stained With Hematoxylin Only

Mitsuyoshi, Tashiro, MS¹
(tashiro.m.ac@m.titech.ac.jp), Rie Yoshida¹,
Tomokatsu Miyazawa¹, Yuri Murakami¹, Masahiro
Yamaguchi¹, Nagaaki Ohyama¹, Yukako Yagi²;
¹Tokyo Institute of Technology, Tokyo, Japan,
²Department of Pathology, Massachusetts General
Hospital, Boston, MA

Content:

Recently multispectral image (MSI) analysis has been developed and expected as a validity tool for pathological diagnosis support. Some methodologies of digital staining for pathological tissue samples were proposed using spectral information. We confirmed tendency of spectral changes between nuclear and cytoplasm tissue in a same single stained slide. Then in this paper, a digital staining method is proposed for producing Hematoxylin and Eosin (H&E) stained image from a specimen stained with Hematoxylin only (H-only).

Technology:

In the digital staining, the transmittance spectrum is estimated from MSI, and the amount of dye is calculated based on Beer-Lambert law, for each pixel from H-only stained tissue. At this time, the spectral absorption coefficients (SAC's) of H pigment in nucleus and cytoplasm are considered to be different. Thus we measure SAC's of H dye in both nucleus and cytoplasm, and apply least mean technique for estimation of the dye amount of each element. In reproducing scheme, the SAC of Eosin is used instead of H in cytoplasm, and the spectral absorbance of digitally stained image is calculated based on the Beer-Lambert law. Then we can obtain the spectral transmittance of the H&E digitally stained image, and a color image is obtained with using the color matching function of human vision.

Design:

In this experiment, a multispectral imaging system was utilized to capture the 16-band image in 2000 x 2000 pixels. The system is composed of a CCD camera, 16 band rotation filters, a conventional optical microscope Olympus BX-62 with an objective lens of 20 fold where the light source is a halogen lamp, and a PC based image capturing and displaying unit. Specimens stained with H only were captured by this system and the proposed technique was applied to the 16-band images.

Result:

In preliminary experiments, we compared the dye amount images of H only and H&E stained image. The result shows the tendency of dye amount images

are similar. Then a color image of H&E digital staining was generated from the dye amount images of H in nucleus and H in cytoplasm.

Conclusion:

We proposed a H&E digital staining method from H-only stained tissue and the result shows the possibility of the digital staining technique.

Utilizing caGrid Infrastructure for Tissue Microarray Analysis

Alex Wright¹, Tony Pan, MS ScB³
(tcpan@emory.edu), Jason Lander², Shiv Kaushal²,
Ashish Sharma³, Joel Saltz, MD, PhD³, Philip Quirke¹,
and Darren Treanor MB BSc, MD¹; ¹Section of
Pathology and Tumour Biology, Leeds Institute of
Molecular Medicine, University of Leeds, United
Kingdom, ²National Grid Service, University of Leeds,
United Kingdom, ³Center For Comprehensive
Informatics, Emory University, Atlanta, GA

Content:

The National Cancer Institute (NCI) Cancer Biomedical Informatics Grid (caBIG[®]) program and the National Cancer Research Institute (NCRI) in the UK are collaborating on the creation of interoperable Grids for sharing data and computing power to facilitate international cancer research. In this abstract we report on the development of a caBIG caGrid-based environment at University of Leeds and its application to facilitate Grid-enabled analysis of TMA images.

Technology:

Tissue microarrays (TMAs) are commonly used in biomedical research. They provide a high-throughput technology for analysis of large number of tissue samples. Scoring TMAs is a time consuming manual process, frequently performed in single site laboratories using microscopes, glass slides, and paper. Grid technology and use of virtual slides for TMAs can facilitate 1) more efficient sharing of images and results; 2) collaborative scoring of TMAs (e.g., by 2 expert pathologists at different institutions); and 3) cooperative development and evaluation of image processing algorithms.

Design:

At University of Leeds, we have employed the caGrid middleware to implement a Grid service for a pixel-based MATLAB[®]. This algorithm detects and quantifies DAB and hematoxylin stained pixels in tissue cores, outputting the percentage of positive stained pixels in the core. caGrid service interfaces allow remote invocation of the pre-compiled algorithm. The analysis outputs are stored locally and accessible to the researcher via a caGrid retrieval interface.

Results:

Remote clients can submit whole-slide TMA images to the caGrid-enabled implementation of the MATLAB® stain quantification algorithm for analysis. The service is being deployed at the UK NGS grid at University of Leeds and Emory University to create a test bed Grid environment.

Conclusions:

Studies involving TMA analyses can benefit from Grid technologies to process images much faster, by using combined processing power across multiple sites, and to analyze multiple images simultaneously. In addition, the computing grid can allow a researcher to utilize diverse image sources in the environment, provide access to a broader set of analytical algorithms, and enable systematic management and collaborative access to analysis outputs.

Analysis of the Visual Search Characteristics of Pathology Residents Reading Digital Slides

Claudia Mello-Thoms, PhD (mellothomsc@upmc.edu), Olga Medvedeva, MS, Eugene Tseytlin, MS, Rebecca Crowley, MD, MS; Department of Biomedical Informatics, University of Pittsburgh, Pittsburgh, PA

Context:

Visual search is an important component of the diagnostic decision making process of pathologists, and significant differences in visual search strategy may lead to different diagnoses on the same case.

Technology:

An intelligent tutoring system (SlideTutor) was used to teach pathology residents to diagnose subepidermal blisters. Residents were initially presented with the digital slide at low power and used a mouse to zoom in on areas of interest, up to 3 magnification levels. At any magnification level residents could move the slide inside the viewing window. Residents marked and named diagnostic features. Cases could be read independently or with aid, through the use of a multi-level hinting-system.

Design:

21 Pathology residents read a case set of 20 subepidermal vesicular dermatitis digital slides using SlideTutor. Residents read the cases over a period of 4 hours. If they concluded the reading sooner, cases started to repeat. We assessed inter- and intra-reader variability by either pairing different residents (inter-reader) or by pairing the two readings of the same case for the same resident (intra-reader) and (1) plotting the viewing window location across the 3

different magnification levels and the low power image, (2) subtracting the two images and (3) calculating the normalized residual area of the difference. Statistical analyses were used to determine whether significant differences ($p < 0.05$) existed in the readers' visual search behavior. Users that relied too much on hints were excluded from analysis.

Results:

Residents do very little exploration at high power and mostly magnify areas that attracted their attention at low power. Preliminary analysis of the data indicates that inter-reader variability was moderately low. If confirmed, this suggests that, at this level of expertise, readers develop a 'standardized' way of analyzing slides, without many personal differentiations.

Conclusions:

Analysis of the visual search characteristics of pathology residents reading dermatopathology slides indicates that residents tend to explore very little of the slide at higher magnifications, instead seeming to prefer to zoom in on the areas that attracted visual attention at low power. This leaves most of the slide unexplored by visual attention.

Tissue Microarray Facilitated Mechanical Characterization of Cancerous Breast Tissue Using Atomic Force Microscopy

Rajarshi Roy, BS¹ (rroy12@umd.edu), Wenjin Chen, PhD²; Jun Hu²; Lauri Goodell²; David J. Foran, PhD²; Jaydev P. Desai¹; ¹Department of Mechanical Engineering, University of Maryland, ²Department of Pathology and Laboratory Medicine, Robert Wood Johnson Medical School, University of Medicine and Dentistry of New Jersey, New Brunswick, NJ

Content:

Atomic force microscopy (AFM) is an emerging tool in biology. Using its unique nano-indenter AFM measures the elastic characteristics of biomedical materials. It has been shown to be sensitive to the presence of disease in cultured cells. In this pilot study we investigated the use of AFM to perform mechanical characterization of fixed breast tissue sections. A tissue microarray configuration was adopted in the experimental design to facilitate accurate sampling using an AFM probe.

Technology:

The AFM system consists of a micro-cantilever (Novascan Technologies Inc., Ames, IA, USA) of stiffness 2.5 N/m that is piezoelectrically controlled to deform tissue samples by a fixed amount (250 nm or

500 nm). Deformation in the sample causes the cantilever to deflect, which is optically sensed by a laser beam reflected from the back of cantilever. This deflection is related to the stiffness of the tissue probed by the AFM.

Design:

Two adjacent breast cancer tissue microarray slices, A and B, were sectioned from a microarray block and fixed onto glass microscopic slides. Slide A was stained with H&E and scanned using a high-resolution Trestle/Zeiss whole-slide imaging device. Resulting digital images were annotated by a board-certified anatomic pathologist to generate a template which would later be used to guide AFM sampling on slide B. This design allowed accurate probing for specific tissue components throughout the complex cancer tissue architecture.

Results:

These experiments showed that cancer tissue exhibited less stiffness than normal tissue, and that epithelial regions exhibited less stiffness than stromal regions. Statistical differences were highly significant. Cancer epithelial regions were significantly softer than non-cancer epithelial regions, which agreed with previous *in vitro* studies.

Conclusion:

Preliminary feasibility studies indicate that AFM can be used to objectively distinguish between normal and cancerous tissue and in discriminating among different subclasses of tissue in both cancer and benign specimens. One of the appealing aspects of the technology is that it does not require specialized staining or preparation of the tissues under examination. In the next stage of research we plan to build a prototype platform to investigate the use of this approach for performing high-throughput analysis and characterization of pathology specimens.

Unified Modeling of Image Annotation and Markup

Fusheng Wang, PhD¹ (fusheng.wang@emory.edu), Tony Pan¹, Tahsin Kurc¹, Ashish Sharma, Joel Saltz, MD, PhD¹, Wenjin Chen, PhD², Vicky Chu², Jun Hu², Lin Yang², David J. Foran, PhD²; ¹Center for Comprehensive Informatics, Emory University, Atlanta, GA, ²Center for Biomedical Imaging & Informatics, The Cancer Institute of New Jersey, New Brunswick, NJ

Content:

We report our progress on the development of a unified image markup and annotation model to standardize observational and computational descriptions of image features for both radiology and pathology/microscopy images. The objective is to

develop a generic and unified data model that enables both syntactic and semantic interoperability for sharing image interpretations in healthcare and clinical trial environments.

Technology:

Image annotation and markup on microscopy images differs from the one on radiology images in several ways: i) more complex microenvironment structures with biological and spatial relationships; ii) different image metadata and additional specimen information; iii) annotations at multiple granularities; iv) new pathology concepts and measurements, and v) more complex geometric shape types for representing pathology annotation targets. We develop the data model through adjusting and extending the caBIG Annotation and Image Markup (AIM) data model, and integrating the Core component developed from ImageMiner data model. We leverage NCI Enterprise Vocabulary Service to describe semantic pathology and biology concepts for annotations.

Design:

The data model consists the following major components: ImageReference, ImageProvenance (the set of information that describes the source of the image, including specimen, equipment, patient, user, group, and the anatomic hierarchy), Annotation (annotation on a target within the image), and AnnotationProvenance (the data analysis process that generates the annotation or markup). An Annotation consists of markup, geometry, feature and assessment, and relationships to other Annotations. AnnotationProvenance captures algorithm and its parameters which generate the annotation results. Attributes used for features and assessments majorly come from the vocabulary, and can also be user defined.

Results:

We have performed a requirement analysis based on a variety of use cases, including tissue microarrays and TCGA Glioblastoma, and developed a preliminary conceptual data model. We are currently aligning the model to AIM and adjusting AIM with revised structures and several new classes.

Conclusions:

Extending AIM data model to support pathology/microscopy not only provides immediate benefit on sharing image information, but also bridges the gap between radiology imaging community and pathology imaging community. Our initial work provides a starting point. Community use cases and requirements are needed for the enrichment of the data model.

Image-based Risk Score: A Computer-Aided Prognosis System for ER+ Breast Cancer Histopathology

Ajay Basavanhally, BS¹
(abasavan@eden.rutgers.edu), Jun Xu, PhD¹; Anant Madabhushi, PhD¹, Shridar Ganesan, MD, PhD²;
¹Department of Biomedical Engineering, Rutgers University, Piscataway, NJ, ²The Cancer Institute of New Jersey, University of Medicine and Dentistry of New Jersey, New Brunswick, NJ

Content:

The gene-expression based Oncotype DX assay is widely used to help determine the prognosis and guide treatment of early stage, estrogen receptor-positive breast cancers (ER+ BC). Although the Oncotype DX Recurrence Score (RS) is correlated with likelihood of distant recurrence and expected benefit from adjuvant chemotherapy, it suffers from translational limitations including a high cost per assay and a long delay between biopsy and prognosis. In this study, we present an Image-based Risk Score (IbRiS) to predict disease outcome and guide treatment for ER+ patients based solely on image-based features from H & E stained histopathology.

Technology:

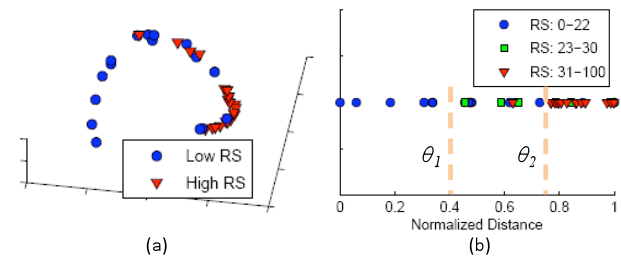
A total of 41 anonymized H&E stained histopathology images were obtained from ER+ BC patients along with corresponding RS values from The Cancer Institute of New Jersey. All samples were digitized via a whole-slide scanner at 20x optical resolution and analyzed with the Matlab software package.

Design:

An automated nuclear detection scheme is first applied to find the centroid of each BC nucleus. Treating the nuclear centroids as vertices, two graphs (Delaunay Triangulation and Minimum Spanning Tree) are constructed. A total of 12 architectural features, such as mean Delaunay triangle area and mean Minimum Spanning Tree edge length, are calculated from these graphs to quantify the spatial arrangement of BC nuclei. Graph Embedding (GE), a non-linear dimensionality reduction technique, is used to reduce the architectural features into a low-dimensional space (see figure below). The IbRiS system is formed by starting at one end of the GE manifold and finding the next nearest image via the Euclidean distance metric. These images are mapped onto a linear scale (see figure below) and this "unraveling" process is continued until all images are included. Prognostic thresholds such as \square_1 and \square_2 can be learnt from training data to predict patient outcome and guide therapy similar to RS on new, independent data.

Results:

The 3-dimensional GE manifold and the resulting IbRiS scale are shown in the figure below. Each data point represents an image, and proximity between images denotes similarity in the feature space. The GE curvilinear data manifold in reduced dimensional space which describes the spatial relationship of the different BC nuclei (and hence disease patterns), where patients with low and high risk of disease progression fall on the extrema of the manifold and the remaining patients fall in between on a continuum of risk. Furthermore, randomized 3-fold cross-validation via a Support Vector Machine classifier demonstrates classification accuracy of $84.15\% \pm 3.10\%$ for discriminating between images with low and high RS.



This figure shows (a) a smooth, continuous manifold emerges when histopathology images are plotted in a reduced 3-dimensional architectural feature space. (b) The IbRiS scale is constructed by using the Euclidean distance metric to unravel (a) and prognostic thresholds \square_1 and \square_2 can aid clinicians.

Conclusion:

IbRiS is a quantitative and reproducible prognostic metric that uses only image-based features from digitized H & E stained histopathology images. It can serve as a fast, inexpensive method to classify ER+ BC that correlates well with validated gene-expression based assays. The IbRiS system includes an algorithm for automatically detecting BC nuclei, architectural features that exploit differences in the spatial arrangement of BC nuclei, and the utility of GE in reducing the architectural features into a single IbRiS value.

Use of Digital Image Capture System with Annotation and Measurement Capabilities in Anatomic Pathology: Technical Design, Benefits and Challenges

Gaurav Sharma, MD, Dhananjay Chitale, MD, Joseph Mark Tuthill, MD (mtuthill1@hfhs.org);
Department of Pathology and Laboratory Medicine, Henry Ford Hospital, Detroit, MI

Context:

Accurate description of gross appearance and measurements of surgically resected specimens is an integral part of anatomic pathology reports. Gross photographs with annotation of sections and diagrams provide invaluable information during review of slides and re-sampling of specimens. For certain specimen types (example breast lumpectomy) entire specimen may be submitted and topographic information is needed for location of lesion and status of margins. Considerable interobserver variability exists in quality and annotation on images and diagrams. We implemented a user-friendly, high-resolution automated digital image capture system (ADICS) with the aim of providing accurate easily accessible information for pathologists.

Technology:

Laboratory Information System (LIS): Sunquest CoPathPlus, Ver 4.0 (Sunquest Information Systems, Tucson, AZ) ADICS: MacroPath D (Milestone S.r.l. Sorisole, Italy) on Intel Pentium 4 (2.2 GHz, 60 GB hard disk) with Windows XP Professional (Microsoft, Redmond VA).

Design:

Pre implementation, specimen images were captured using digital cameras at the grossing stations and diagrams with section annotations were hand drawn and manually scanned. These were uploaded to a network shared drive in case specific folders and accessed by pathologists at the time of case sign-out. Measurements and gross descriptions were dictated in the report. Post implementation, specimen images were captured on ADICS and the sections and measurements were annotated on system screen. The original image and copies with annotations and measurements were automatically saved in case specific folders.

Results:

ADICS combined 6 processes including hand-drawing diagrams, scanning, creating folders and uploading images case folders (example: 15-20 minutes for a lumpectomy) and reduced the number of lost images. High quality annotated images provided better topographical information on size and location of lesion with margins and aided re-sampling if needed.

Conclusion:

Single process by ADICS with annotation abilities dramatically reduced the turnaround time at the grossing station with improved efficiency. The benefits of implementing this system in a high volume surgical pathology laboratory outweigh the investment, improve workflow and provide accurate, accessible gross examination information to pathologists complementing final reports including future teaching and clinical purposes. Challenges

include the initial capital/ maintenance cost and user training time.

Her-2 Signal Enumeration in FISH Image Stacks in Invasive Breast Cancer Specimens

Michael W. Kilpatrick, PhD
(Kilpatrick@ikonisys.com), Changhua Yu, Xiuzhong Wang, Triantafyllos Tafas; Ikonisys, Inc. New Haven, CT

Content:

To determine Her-2 status in invasive breast cancer specimens, accurate automated FISH dot counting is highly desirable. Various intensity-based thresholding techniques have been developed for dot segmentation in FISH images. Here we present a gradient-based dot detection method. The proposed method is verified by analysis of several breast cancer slides.

Technology:

Specimen slides were prepared, hybridized with two FISH probes, an orange Her-2 probe and a green control probe and counterstained with Dapi. Slides were imaged in all 3 fluorescence channels, Dapi, orange and green, using an automated epifluorescence microscope equipped with a 100x objective.

Design:

Nuclei are segmented based on the DAPI image and, using the segmented nucleus DAPI mask, the FISH channel cutout stacks of each nucleus are generated. The best focal plane is identified and 5 planes around the best focal plane are then chosen for dot counting. Before searching for FISH signals, top-hat filtering is used to reduce noise introduced by fluorescent residue. Adaptive thresholds are found based on maximum gradient images. Pixels with gradient above threshold grow into dots. Finally, FISH signals are recognized by a trained multi-layer perceptron (MLP) utilizing the 3D features of size, shape and intensity.

Results:

Five breast cancer slides were used to evaluate the automated FISH signal detection method. For each slide, at least 100 nuclei were analysed. The dot feature samples from 2 slides were used for MLP training and samples from the remaining slides were used for testing. Trained personnel manually counted and tabulated the FISH signal in each nucleus. The agreement between automated and manual FISH signal counting for the slide set ranged from 80.26% - 91.15%.

Conclusions:

We have proposed a gradient-based method for the detection of FISH signals using a monochrome FISH image stack. In the 3D image stack, pixels with gradient magnitude above adaptive thresholds grow into dots. Shape, area and relative volume features are extracted. Normalized intensity features reflecting local contrast are also used. A three-layer MLP is trained to discriminate the FISH signals. Experimental results with breast cancer specimen slides demonstrated the automated dot counting ability of the proposed method.

One-Stage and Two-Stage Models for Compressing Pathology Image Slides

Sourabh Khire¹, Saunya M. Williams¹ (saunya@gatech.edu), Nikil Jayant, PhD¹, Alexis B. Carter, MD², Uday Srinath¹; ¹School of Electrical and Computer Engineering, Georgia Institute of Technology, Atlanta, GA, ²Department of Pathology and Laboratory Medicine, Emory University, Atlanta, GA

Context:

While mathematical losslessness (ML) in image compression provides maximum fidelity in digital pathology, pervasive digital practice may need a higher level of compression. To this end, we proposed the criterion of diagnostic losslessness (DL) at APIII 2008, with expert-specified diagnostic quality guiding the degree of compression. We extended the DL-idea, focusing on the total bits needed for digitizing pathology images in the alternative approaches of one-stage and two-stage compression.

Technology:

SPOT Digital Cameras (Diagnostic Instruments, Inc) were used to capture uncompressed images from slides of morphologically distinct lesions. Multiple versions of each digital photomicrograph were created using JPEG and JPEG 2000.

Design:

To create a workflow model, we defined another level of compression: Perceptual losslessness (PL), which is not as stringent as DL, but provides adequate image quality to locate a region of interest (ROI) in a pathology image or to identify prominent within-ROI features. As a pilot study, one pathologist annotated images with ROIs needed for diagnosis. Two levels of magnification, low (XL) and high (XH), as well as the fractional area F of the ROI in an image were postulated and applied to two models: (1) a 1-stage model where the entire image is represented at XH and compression level of DL, and (2) a progressive 2-stage model where (i) the entire image is represented at XL and at the compression level PL (preserving ROI), followed by (ii) a second stage where the ROI is

represented at XH and compression level of ML (or DL). The bit-efficiencies of the models are compared as a function of ML, DL, PL, XH, XL and ROI fraction F.

Results:

Analytical results were obtained for the number of bits needed (and therefore the time taken) to represent a digital slide in each model. For ML= 2:1, DL =10:1, PL=60:1, XH=40x, and XL=10x, the 1-stage model was seen to be bit-rate-competitive with, but not always more bit-efficient than, the inherently economical 2-stage model, depending on the ROI fraction F.

Conclusion:

The 1-stage model is viable from an information viewpoint, while offering better workflow by not needing expert intervention for ROI detection.